Selective Anchoring in the Specific Plasma Membrane Domain: A Role in Epithelial Cell Polarity

Pedro J. I. Salas,* Dora E. Vega-Salas,* Jerome Hochman,‡ Enrique Rodriguez-Boulan,* and Michael Edidin‡

*Department of Cell Biology and Anatomy, Cornell University Medical College, New York 10021; and
‡Department of Biology, Johns Hopkins University, Baltimore, Maryland 21218

Abstract. We have studied the role of restrictions to lateral mobility in the segregation of proteins to apical and basolateral domains of MDCK epithelial cells. Radioimmunoassay and semiquantitative video analysis of immunofluorescence on frozen sections showed that one apical and three basolateral glycoproteins, defined by monoclonal antibodies and binding of beta-2-microglobulin, were incompletely extracted with 0.5% Triton X-100 in a buffer that preserves the cortical cytoskeleton (Fey, E. G., K. M. Wan, and S. Penman. 1984. *J. Cell Biol.* 98:1973–1984; Nelson, W. T. and P. J. Veshnock. 1986. *J. Cell Biol.* 103:1751–1766). The marker proteins were preferentially extracted from the "incorrect" domain (i.e., the apical domain for a basolateral marker), indicating that the cytoskeletal anchoring was most effective on the "correct" domain. The two basolateral markers were unpolarized and almost completely extractable in cells prevented from establishing cell–cell contacts by incubation in low Ca^{++} medium, while an apical marker was only extracted from the basal surface under the same conditions.

Procedures were developed to apply fluorescent probes to either the apical or the basolateral surface of live cells grown on native collagen gels. Fluorescence recovery after photobleaching of predominantly basolateral antigens showed a large percent of cells (28–52%) with no recoverable fluorescence on the basal domain but normal fluorescence recovery on the apical surface of most cells (92–100%). Diffusion coefficients in cells with normal fluorescence recovery were in the order of 1.1×10^{-9} cm^2/s in the apical domain and $0.6–0.9 \times 10^{-9}$ cm^2/s in the basal surface, but the difference was not significant. The data from both techniques indicate (*a*) the existence of mobile and immobile protein fractions in both plasma membrane domains, and (*b*) that linkage to a domain specific submembrane cytoskeleton plays an important role in the maintenance of epithelial cell surface polarity.

THE polarization of plasma membrane proteins into apical and basolateral domains is key to vectorial function of epithelia (60, 70). Recent work with the MDCK cell system has demonstrated two mechanisms that contribute to this surface polarity: (*a*) sorting by the *trans*-Golgi into carrier vesicles which are then vectorially delivered to the correct domain (10, 41, 45, 55, 58, 64), and (*b*) the tight junctional fence (16). It seems now quite clear that tight junctions may segregate lipids in the outer leaflet of the bilayer (17, 81) but the extent of their contribution to protein segregation is still unknown. Thus, although dissociation of tight junctions with calcium chelating agents results in the invasion of the apical and basolateral regions by markers previously segregated (29, 56, 88), other Ca^{++}-dependent cell adhesion molecules, junction adhesion molecules, and substrate adhesion molecules are also disrupted by the same treatment (21, 52, 75). In addition, some apical membrane proteins are polarized in MDCK cells with incomplete tight junctions (82), which indicates that restrictions to lateral diffusion other than complete tight junctions are involved in the maintenance of epithelial surface polarity. This result raised the question of whether restrictions to lateral diffusion within the plane of the membrane or interdomain fences play a significant role in the maintenance of epithelial surface polarity.

Recent work has highlighted the role of specific protein–protein interactions in the retention of markers characteristic of the endoplasmic reticulum and Golgi apparatus (39, 53), raising the possibility that specific retention of membrane proteins at their correct domain may play a significant role in sorting mechanisms (62). Furthermore, components of the erythroid submembrane cytoskeleton, spectrin and ankyrin, which restrict the lateral mobility of red cell membrane proteins (5, 9), have been recently described in association with the basolateral surface of kidney tubules and MDCK cells (19, 48). In this work, we have

Pedro J. I. Salas and Dora E. Vega-Salas' present address is Instituto de Investigaciones Bioquimicas, Fundacion Campomar, Avenida Patricias Argentinas 435, 1405 Buenos Aires, Argentina.

searched for domain-specific cytoskeletal anchorage of epithelial plasma membrane proteins using two independent approaches: Triton X-100 (TX-100)[1] extractability (1, 2, 3, 6, 8, 11, 67, 78) and fluorescence recovery after photobleaching (22, 23, 32). The results indicate that specific immobilization in their correct domain can account for the maintenance of polarity of important fractions (i.e., 30–90%) of one apical and three basolateral MDCK cell membrane proteins.

Materials and Methods

Antibodies and Probes

Detailed procedures have been described elsewhere (82, 83). Briefly, monoclonal antibodies against MDCK cell surface antigens were obtained by intraperitoneal immunization of BALB/c mice with MDCK cell monolayers grown on beads, alternating fixed and live cells in bi-weekly successive injections. Then spleen lymphocytes were fused with NS-1 myeloma cells (35) and the supernatants from resulting hybridomas were tested for anti-MDCK cell surface binding activity. Monoclonal antibodies against apical and basal markers were characterized by immunofluorescence on semi-thin frozen sections and immunoblot. Their Ig subtype was analyzed by the agar immunodiffusion test, using Ig subtype specific antibodies (Boehringer Mannheim Biochemicals, Indianapolis, IN).

Fab fragments were prepared from two monoclonal antibodies as described elsewhere (22). Briefly, the Igs were purified by precipitation with 40% $(NH_4)_2SO_4$ followed by DEAE-cellulose ion exchange chromatography and dialyzed against 0.15 M NaCl, 0.001 M Na_2 EDTA, 0.1 M potassium phosphate, pH 8.0. Then, 5 mg Ig (2 ml) were incubated with 40 U of 2× crystallized papain (Sigma Chemical Co., St. Louis, MO) previously activated for 15 min at room temperature in 0.1 M sodium acetate, 0.01 M cysteine, and 0.001 M EDTA buffer. The digestion was stopped by adding solid iodoacetamide up to a final concentration of 0.05 M. The papain digest was dialyzed against 0.5 M sodium carbonate buffer, pH 9.0, conjugated with FITC (Research Organics, Inc., Cleveland, OH) for 2 h and further dialyzed against a large excess of PBS. Undigested Ig, Fab fragments, and free dye were separated by chromatography on a Sephadex G-100 column (1.5 × 50.0 cm). Fractions corresponding to the second peak, which contained most of Fab, as determined by SDS-PAGE, were collected and rechromatographed once to eliminate all undigested antibody. Conjugates with a fluorescein/protein ratio of ~1.0 were tested by indirect immunofluorescence on formaldehyde-fixed MDCK monolayers, concentrated by dialysis against solid polyvinyl pyrrolidone (mol wt = 40,000; Sigma Chemical Co.) and stored at −20°C.

FITC-conjugated human beta-2-microglobulin (B2-m) was prepared from urine (30) and substituted with 1 mol of fluorescein per mol of B-2m. This derivative readily exchanges with endogenous B2-m to label the basolateral surface of MDCK cells. The labeled B2-m is stable, bound with K_D 10^{-8}–10^{-9} M. Less than 20% of bound B2-m dissociates after 60 min of incubation of labeled cells at conditions of "infinite dilution" (30).

Cell Culture

The general tissue culture conditions of MDCK cells have been described before in normal D-MEM (63) as well as the use of low calcium (~5 uM) medium (S-MEM) that results in confluent monolayers with minimal development of cell-cell contacts (27, 82).

Cell Fractionation and Membrane Protein Extraction

Post nuclear supernatants of MDCK cells were obtained from monolayers grown on square (24 × 24 cm) plastic dishes (Nunc Inc., Newbury Park, CA). The cells were scraped with a rubber policeman in PBS/distilled H_2O (1:1) supplemented with 2 mM Na_2 EDTA, 1 mM phenylmethylsulfonyl fluoride (PMSF; Sigma Chemical Co.), 1 mM benzamidine (Sigma Chemical Co.), 1 mM pepstatin (Sigma Chemical Co.), and 0.1 mM aprotinin (scraping buffer; Sigma), passed 50 times through the blue tip of an Eppendorf pipette at 0°C and the resultant homogenate spun at 10,000 *g* for 10 min in a centrifuge (model RC5C; Sorvall Instruments Div., Wilmington, DE) to pellet the nuclei.

To test for cytoskeletal attachment of membrane components, we used a modification of the buffer developed by Fey et al. (25). The monolayers were rinsed twice with extraction buffer (EB): 100 mM KCl, 2 mM $MgCl_2$, 4 mM Na_2 EGTA, 60 mM Pipes (Research Organics, Inc.), pH 6.9; and extracted for 10 min at room temperature with 0.5% TX-100 (Sigma Chemical Co.) in EB, 1 mM PMSF. We found that the addition of EGTA resulted in an excellent preservation of the membrane cytoskeleton. The cytoskeletal preparations were processed for RIA or imunofluorescence. Alternatively, they were removed in scraping buffer, treated with 0.1 mg/ml DNAase I (Sigma Chemical Co.) for 1 h at room temperature, homogenized with 50 strokes of a glass homogenizer (Dounce, Vineland, NJ), exposed to various extraction conditions (see Results), centrifuged at 215,000 *g* for 30 min at 10°C, and processed for indirect RIA on the bottom of the ultracentrifuge tube.

RIA and Immunofluorescence

The procedures for RIA, immunofluorescence on semi-thin frozen sections, and electron microscopy have been described in detail elsewhere (61, 63, 82, 83). Briefly, MDCK cells were plated at immediate confluency on 50-well detachable tissue culture dishes (~100,000 cells per well; Lux, Miles Laboratories, Inc., Naperville, IL) and fixed 24 h later with either 2% formaldehyde (freshly prepared from paraformaldehyde [PFA]) at room temperature, or 96% methanol at −20°C. The monolayers were then sequentially treated with 50 mM NH_4Cl in PBS, 1% BSA (Sigma) in PBS supplemented with 50 μg/ml preimmune goat IgG, mAb, and affinity-purified ^{125}I-goat anti-mouse IgG. The wells were washed, dried, detached, and counted in a gamma counter (Hewlett-Packard Co., Palo Alto, CA).

For labeling with B2-m, cells were incubated and washed as described below (see Fluorescence Recovery after Photobleaching section), fixed in 2% PFA, and processed with a rabbit anti-human B2-m and affinity-purified rhodamine-conjugated goat anti-rabbit IgG.

For frozen sections, MDCK cells were plated on native type I collagen-coated glass coverslips. After fixation with 2% PFA, the monolayers were scraped with a razor blade, placed into 1 × 10-mm molds containing 10% gelatin in PBS at 40°C and transferred to 4°C to allow gelling. The gelatin blocks were infused overnight with 1.8 M sucrose, 0.2% PFA in PBS, frozen in liquid N_2, and sectioned at −85°C with an ultramicrotome (model MT5000; Sorvall Instruments Div.) equipped with an FS-1000 cryoattachment. The sections (~0.5 μm) were collected on 1.8 M sucrose drops, bound to coverslips pretreated with poly-L-lysine (Sigma), and processed for immunofluorescence with mAbs as described above but using affinity-purified rhodamine-conjugated goat anti-mouse IgG (Jackson Immuno Research Laboratories, Avondale, PA). F-actin was labeled with 5 μg/ml rhodamine phalloidin (Molecular Probes, Inc., Junction City, OR). The sections were mounted in polyvinyl alcohol (type Vinol; Air Products and Chemicals, Allentown, PA), observed under a Leitz Ortholux epifluorescence microscope, and photographed with Tri-X 400 ASA film (Eastman Kodak Co., Rochester, NY). For quantitation of fluorescence, the images were collected with a silicon intensified video camera (SIT-66, Dage-MTI, Wabash, MI) and processed as discussed elsewhere (82).

The antibody penetration in the gelatin sections was measured by incubating gelatin blocks (previously fixed in 0.2% PFA) in 1 mg/ml ferritin (Sigma) for 1 h. The blocks were rapidly rinsed in PBS, postfixed in 2% glutaraldehyde, and processed for EM. Ferritin particles were observed to be evenly distributed at 1–5 μm from the gelatin edge, indicating that antibodies, smaller than ferritin in molecular size, penetrate the full thickness of 0.5-μm-thick frozen sections. Therefore, for semi-quantitative measurements of fluorescence on semi-thin frozen sections from detergent-extracted and unextracted cells, the variability in section thickness was measured by the following experiment. 7 μCi of ^{125}I-protein A were dried by vacuum evaporation and resuspended in 10 μl of 10% gelatin in PBS. The gelatin was placed in a 1-mm^2-section mold, hardened in the cold, fixed in 2% PFA, infused in 1.8 M sucrose, and frozen sectioned as described above. Single sections of similar shape were picked up with the tips of wooden rods (one section per rod). Then, the rods were counted in a gamma-counter. 21 consecutive sections showed 184 ± 28 cpm above background. This represents a standard deviation of ±15% in section thickness. To avoid a bias introduced by measuring fluorescence from sections of different thickness, this variability was statistically normalized in detergent extraction experiments: the images were collected from several different sections of both extracted and unextracted samples.

1. Abbreviations used in this paper: B2-m, beta-2-microglobulin; EB, extraction buffer; FRAP, fluorescence recovery after photobleaching; PFA, paraformaldehyde; TIF, totally immobile fraction (percent of spots with no recovery after photobleaching); TX-100, Triton X-100.

The linearity of response was controlled by mixing 10% gelatin with chromatographically pure mouse IgG (Organon Tecknika-Cappel, Malvern, PA) at final concentrations of either 1 or 10 mg/ml. Three layers of gelatin containing 0, 1, or 10 mg/ml mouse IgG were placed together in 1-mm^2-section molds and processed for frozen sections as described above. Sections containing gelatin with the three IgG concentrations were processed for immunofluorescence with affinity-purified rhodamine-coupled goat anti-mouse IgG antibody. The images from these sections were collected as described before and showed levels of fluorescence similar to those observed on MDCK cell plasma membranes labeled with specific monoclonal antibodies. After subtracting the pixel values of the background (gelatin with no IgG) the ratio between the average fluorescence on 10 and 1 mg/ml IgG gelatins was 9.65 indicating that the fluorescence intensities linearly correlate with antibody concentrations.

Since the fluorescence was compared domain by domain (i.e., apical to apical) in unextracted and detergent extracted cells, it was assumed that detergent extraction does not modify the membrane folding and no correction for membrane folding was used. The validity of this assumption was confirmed at the EM level (see Fig. 1 *C*).

Fluorescence Recovery after Photobleaching

The principles and procedures of the fluorescence recovery after photobleaching (FRAP) technique have been discussed before (22, 23, 33).

In this work, FRAP measurements were performed on MDCK cells under three different conditions. (*a*) Adding the fluorescent probes to the apical domain of confluent monolayers. This set of measurements was carried out on cells grown either on glass coverslips or collagen/Nitex filters (see below). No differences were found between both conditions. (*b*) The fluorescent probes were added to the free surface of sparse cells incubated in D-MEM or confluent monolayers prevented from establishing intercellular contacts by incubation in S-MEM on glass coverslips. (*c*) To allow access of probes to the basolateral surface, confluent MDCK monolayers were formed on 15-μm mesh nylon filters (type Nitex; Tetko, Elmsford, NY), glued to acrylic plastic rings, and covered with native type I collagen gels (24). Previous studies (12, 63) have shown that filter grown MDCK cells display 200–300 Ω.cm^2 transmonolayer electrical resistance and are impermeable to antibodies. The cells were plated on the internal chamber at immediate confluency (2–3 × 10^5 cells/cm^2) in D-MEM 10% horse serum, which was changed 2 h later to protein-free, dye-free D-MEM and immediately before the experiment to Moscona's saline solution (140 mM NaCl, 2.7 mM KCl, 4 × 10^5 M, sodium phosphate, 11.9 mM $NaHCO_3$, 9.4 mM glucose) supplemented with 50 mM Hepes (pH 7.5), 0.1 mM $CaCl_2$, 1 mM $MgCl_2$, and 50 μg/ml pre-immune, electrophoretically pure, mouse IgG (washing buffer). After 20 min on ice, fluorescein-conjugated Fab fragments were added to the same medium up to a final concentration of 30 μg/ml. Labeling by B2-m: subconfluent or confluent cells were incubated with 10^{-7} M FITC-B2-m in medium containing 0.1% BSA for 8–12 h and then washed free of excess B2-m. To enhance the fluorescent signal from fluorescent Fab fragment mAb, a fluorescein-conjugated Fab fragment from a goat anti-mouse IgG (Organon Tecnika-Cappel), was occasionally added. In this case, pre-immune mouse IgG was not present in the incubation medium. When the probes were added from the apical side, the total incubation time was 1 h, followed by four washes in washing buffer. When the fluorescent probes were added from the basolateral side, the incubation time was 3–7 h followed by 3 × 1-h washes in washing buffer. Previous studies indicate that the monolayers remain tight under these conditions. These long incubation periods were required to allow diffusion of the antibody through the unstirred layers trapped in the filter (45, 63). All these procedures were performed on ice to prevent endocytosis of the labeled probes. The nylon filters were detached from the plastic ring and the cells were mounted in washing buffer under a glass coverslip facing the microscope objective. FRAP measurements were performed usually at 19°C, immediately after washing away free antibody.

A control was performed labeling the cells with primary Ab and fluorescent anti-mouse Ig Fab. The label was measured by flow cytometry in the presence of a large excess of unlabeled Fab. No significant dissociation was observed in 90 min.

FRAP was performed with the laser beam perpendicular to the apical and basal domains. Most of the measurements of basolateral FRAP were carried out by focusing the laser beam on the center of the cell and therefore mainly estimate the mobility of the basal antigen, although the degree of contribution of lateral antigen cannot be determined. However, it has been shown that membrane folding parallel to the laser beam such as microvilli do not critically affect FRAP measurements (87).

Results

Plasma Membrane Proteins of MDCK Cells Show Differential Extractions in TX-100

In this work, we have used four monoclonal antibodies directed against cellular plasma membrane antigens of MDCK cells. The key features of these antibodies and their antigens are illustrated in Table I. Two of them react with apical membrane proteins (S8/1M13 and S2/2G1) and will be hereafter referred to as A1 and A2, respectively. The other two react with basolateral proteins (S2/3G2 and S7/5G23) and will be referred to as B1 and B2. The antigens for all four of them showed membrane associated fluorescence images in semi-thin frozen sections (see Figs. 3, 4, and 5). A1, B1, and B2 behaved as integral membrane proteins according to both of the following criteria: (*a*) <14% was extractable in 0.1 M Na_2CO_3, pH 11 (26), and (*b*) >70% partitioned with the detergent phase when the cells were extracted with Triton X-114 (reference 7). A2, the best polarized of all four antigens, although resistant to alkali extraction, partitioned preferentially with the water phase during Triton X-114 phase separation. Other integral membrane proteins, including the acetylcholine receptor (40), uvomorulin (28), and the platelet Ib glycoprotein (14) have been shown to behave like A2 during Triton X-114 phase separation. On the other hand, mutants in the p62/E2 protein, an integral membrane protein of Semliki Forest virus have been shown to be an exception to the high pH criterion (15).

The possible anchoring to the cytoskeleton of the four antigens was assayed by extraction of live cells with 0.5% TX-100 in extraction buffer (EB; 100 mM KCl, 4 mM EGTA, 2 mM $MgCl_2$, 1 mM PMSF, 60 mM Pipes, pH 6.9), which maximizes preservation of the MDCK submembrane cytoskeleton. As described by Fey et al. (25), the extracted cells

Table I. Characterization of Monoclonal Antibodies against Cellular Plasma Membrane Antigens of MDCK Cells

mAb		Cellular antigen			
				Antigen after extraction	
Name	Type	M_r	Periodate sensitivity	TX-114 phase (in percent)	pH 11 (in percent)
		kD			
S8/1M13 (A1)	IgM	215	YES	74	98
S2/2G1 (A2)	IgG1	184	NO	20	87
S2/3G2 (B1)	IgG1	63	NO	70	92
S7/5G23 (B2)	IgG2b	49	NO	80	86

The antibody type was determined by agar immunodiffusion assay against specific antibodies. M_r was determined by immunoblots from SDS-PAGE of MDCK cell postnuclear supernatants. Some supernatants were treated with 50 mM sodium periodate and then assayed by immunoblot. Triton X-114 extractability: MDCK cell monolayers were extracted at 0°C in 0.5% Triton X-114, the detergent phase was spun at 37°C, and resuspended/spun twice. The proteins in the detergent phase were assayed by SDS-PAGE and immunoblot. The specific bands were cut and counted. The 100% was calculated as the cpm in the specific band from an SDS extract obtained from the same number of cells. pH 11 extraction: MDCK cell postnuclear supernatants were incubated in ice-cold 0.1 M Na_2CO_3, pH 11.0, or in PBS, pH 7.5, (control) for 30 min (26). The membranes were spun for 1 h at 100,000 *g*, and each membrane protein was determined by SDS-PAGE and immunoblot. The specific bands were cut and counted (100%: untreated membranes).

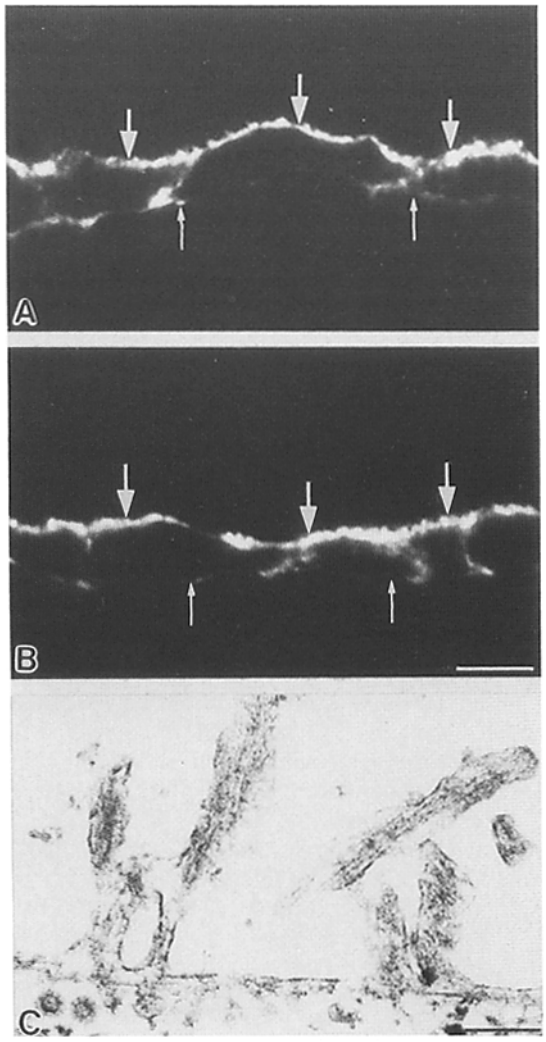

Figure 1. Morphology of MDCK cell submembrane cytoskeleton after extraction with TX-100. MDCK cells were plated at immediate confluency and incubated for 2 d. Some monolayers were extracted in 0.5% TX-100 in EB (*B* and *D*) and then fixed in 2% PFA (for fluorescence) or 2% glutaraldehyde (for EM). The semi-thin (0.5 μm) frozen sections were processed with rhodamine-coupled phalloidin. (*A*) Distribution of phalloidin binding sites in an unextracted monolayer. *Large arrows*, apical; *small arrows*, basal. (*B*) Phalloidin binding sites after TX-100 extraction. (*C*) EM of the apical domain of TX-100-extracted cells. Bars: (*A* and *B*) 9.4 μm; (C) 0.15 μm.

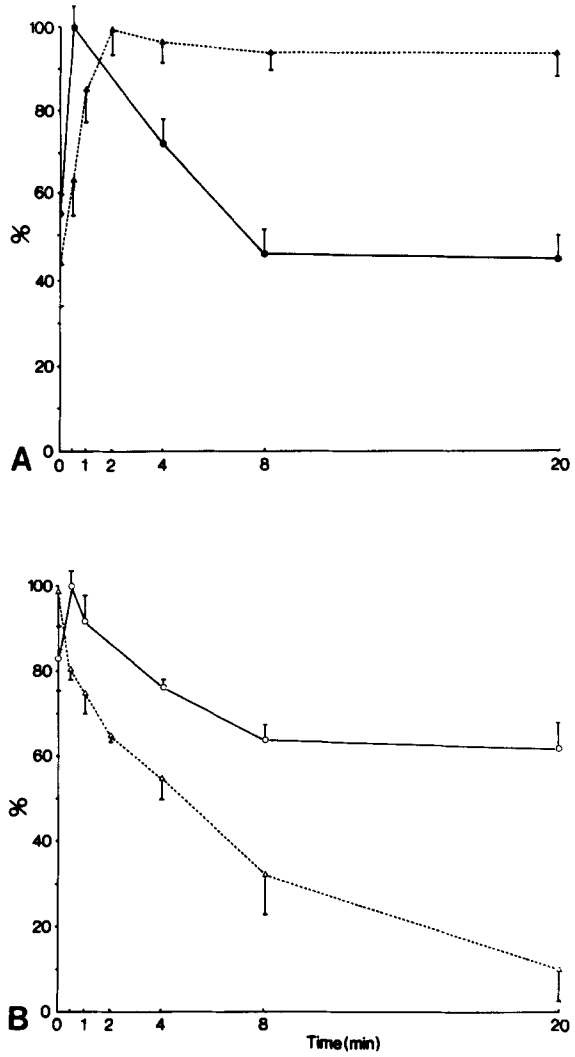

Figure 2. RIA determination of MDCK plasma membrane proteins during Triton X-100 extraction. MDCK cells were plated at immediate confluency in 50-well detachable Petri dishes (~10^5 cells per well) and incubated for 1 d. The cells were fixed at various times after addition of 0.5% TX-100. The monolayers were processed for indirect RIA with the monoclonal antibody markers and affinity-purified ^{125}I-goat anti-mouse IgG. The data are shown as mean ± SD of five measurements considering the maximum value for each marker as 100% (typically 1–2 × 10^4 cpm per well above background). (*A*) Basolateral markers, B1 (●) and B2 (▲). (*B*) Apical markers, A1 (○) and A2 (△).

kept to a large extent the nonextracted cell shape at the phase contrast and EM levels. In agreement with previous observations (18, 44), an actin-rich submembrane cytoskeleton was observed associated with both apical and basolateral surfaces of MDCK cells by rhodamine phalloidin fluorescence on semi-thin frozen sections; larger amounts of actin were detected on the apical surface due to the presence of microvilli (Fig. 1 *A*). As shown by other groups (25, 31, 43), TX-100 in EB failed to extract F-actin (Fig. 1 *B*) and preserved the ultrastructural features of the cortical cytoskeleton including microvilli (Fig. 1 *C*).

The time course of the extraction by TX-100–EB of the four MDCK antigens was studied in monolayers plated for 24 h by RIA with monoclonal antibodies (Fig. 2). The binding of both B1 and B2 monoclonals increased during the initial 30 s, presumably due to increased antibody accessibility to the basolateral domain, followed by a 50% decrease, for B1, or a slight 5% decrease, for B2, during the next 10 min (Fig. 2 *A*). At this time a plateau was reached. The apical protein A1 displayed similar biphasic extraction kinetics, presumably due to some intracellular and basolateral localization (Fig. 2 *B*; see also Fig. 3 *C*); the maximum level of extraction, 40% of the peak value, was reached after 10 min. On the other hand, A2, which is exclusively distributed on the apical plasma membrane in confluent monolayers with normal cell–cell contacts (82, 83), was continuously extracted to <10% of the initial signal (Fig. 2 *B*). Using the same protocol the total cellular extractability in TX-100 was

assayed in 4-d confluent MDCK monolayers. The TX-100-extractable fractions in steady-state were similar to those shown in Fig. 2: A1, 24%; A2, 90%; B1, 36%; and B2, 10%.

Even though the total amount of basolaterally distributed antigens was underestimated in these experiments because antibodies did not reach the basolateral domain before detergent was added, these results indicate that significant fractions of A1, B1, and B2 remain attached to the MDCK cytoskeletal preparation after addition of 0.5% TX-100 in EB.

Plasma Membrane Proteins Are Preferentially Extracted from the "Incorrect" Domain

To study the distribution of the TX-100-insoluble and -soluble fractions, MDCK cell monolayers were extracted, fixed, frozen sectioned, and processed for immunofluorescence with A1 and B1 monoclonals (Fig. 3). Both markers showed a relatively "imperfect" polarity with small but detectable levels of mAb binding to the "incorrect" surface (i.e., the basolateral surface for an apical marker; Fig. 3, *A* and *C*, *arrows*). The extraction with TX-100 resulted in the disappearance of B1 fluorescence from the apical surface and of A1 fluorescence from the basolateral plasma membrane domain (Fig. 3, *B* and *D*, *arrows*). Strikingly, antigen in the correct domain was relatively unextracted, suggesting binding to the submembrane cytoskeleton. Similar results were observed for two more basolateral markers: B2 and B2-m, the physiological endogenous light chain of class I major histocompatibility antigens, DLA (not shown).

By counting positive lateral membranes, we found that B1 and B2 mAbs labeled 100% of lateral plasma membranes before detergent extraction. After TX-100 extraction of 24-h-old confluent monolayers, 90% of the cells' lateral membranes were positive with B1 and 100% with B2. This proportion was somewhat smaller for B2 in 4-d-old monolayers: 90 and 79%, respectively. This suggests some heterogeneity in the cell population. Negative membranes were included in statistics for semi-quantitative determination (see below).

These results were semi-quantitated by digital video analysis of fluorescent semi-thin frozen sections, as previously described (82), to avoid the bias introduced by nonlinearity in photographic reproduction. The gain of the video camera was fixed so that the values of the plasma membrane pixels from unextracted and extracted samples fell, for each antigen, within the linear range of sensitivity of the camera. Significant peaks of basal (incorrect domain) fluorescence were found with the A1 marker (Fig. 4 *A*, *arrows*) in randomly taken fluorescence profiles from nonextracted cells; these peaks were abolished in TX-100-extracted monolayers (Fig. 4 *B*, *arrows*). Likewise, basolateral antigens showed some apical fluorescence observed as apical peaks of fluorescence (Fig. 4, *C* and *E*, *black arrows*). After detergent extraction these peaks of fluorescence in the incorrect domain decreased to a greater extent than the peaks in the "correct" domain (Fig. 4, *D* and *F*, *black arrows*).

The size of the detergent-extractable population for each membrane protein in each domain was calculated by comparing the size of fluorescence peaks in digitized images of frozen sections from detergent-extracted and control monolayers. Since antibodies penetrate the full thickness of 0.5-μm frozen sections, we determined the variability in section thickness and found that it was <15%. This variability was statistically normalized by collecting images of several different sections from control and detergent-extracted cells. The linear correlation between antibody concentration and fluorescence intensity was also assayed in parallel controls (see Materials and Methods). The size of the fluorescence peaks was calculated by subtracting the average extracellular fluorescence background (typically 50–90 pixel units; i.e., see Fig. 4, *E* and *F*, *small white arrows*). The extracellular fluorescence was not affected by detergent extraction. The resulting values of extractability in detergent are labeled *E* in Table II. Since this method cannot completely discriminate the contribution of cytoplasmic fluorescence, it

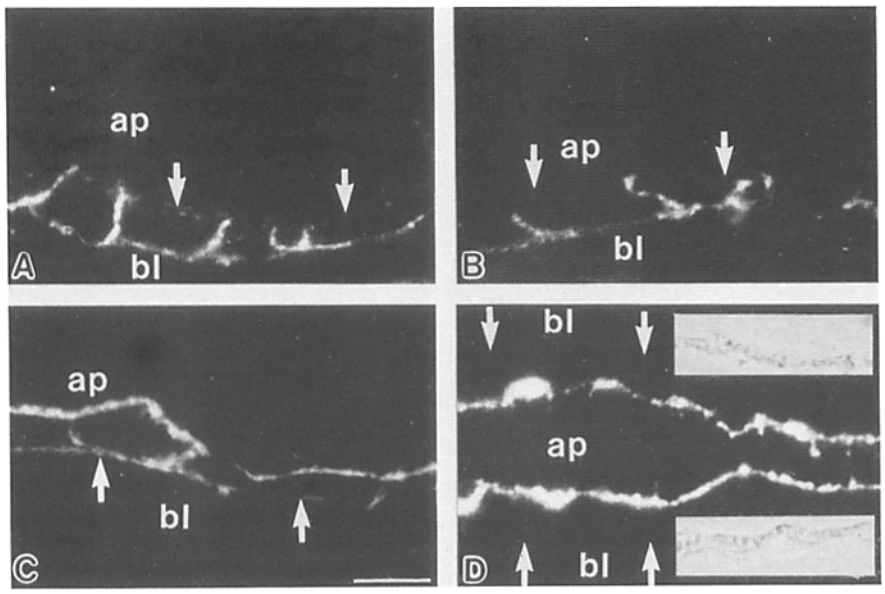

Figure 3. Immunofluorescence localization of MDCK cell plasma membrane proteins in semi-thin frozen sections after TX-100 extraction. MDCK cells were plated at immediate confluency and incubated for 24 h. Some monolayers were extracted in 0.5% TX-100 for 10 min before fixation (*B* and *D*). The monolayers were fixed in 2% PFA, frozen sectioned, and processed for immunofluorescence with the anti-MDCK cell membrane protein monoclonal antibodies B1 (*A* and *B*) and A1 (*C* and *D*). (*A*) B1 MAb, unextracted; (*B*) B1, preextracted in TX-100; (*C*) A1 MAb, unextracted; (*D*) A1, preextracted in TX-100. Note that *D* shows a fold of the monolayer with the apical domains of two adjacent areas facing each other. (*Insets*) Corresponding phase images. The arrowheads show the fluorescence in the incorrect domain (i.e., the basal fluorescence of a mostly apical marker). Bar, 20.7 μm.

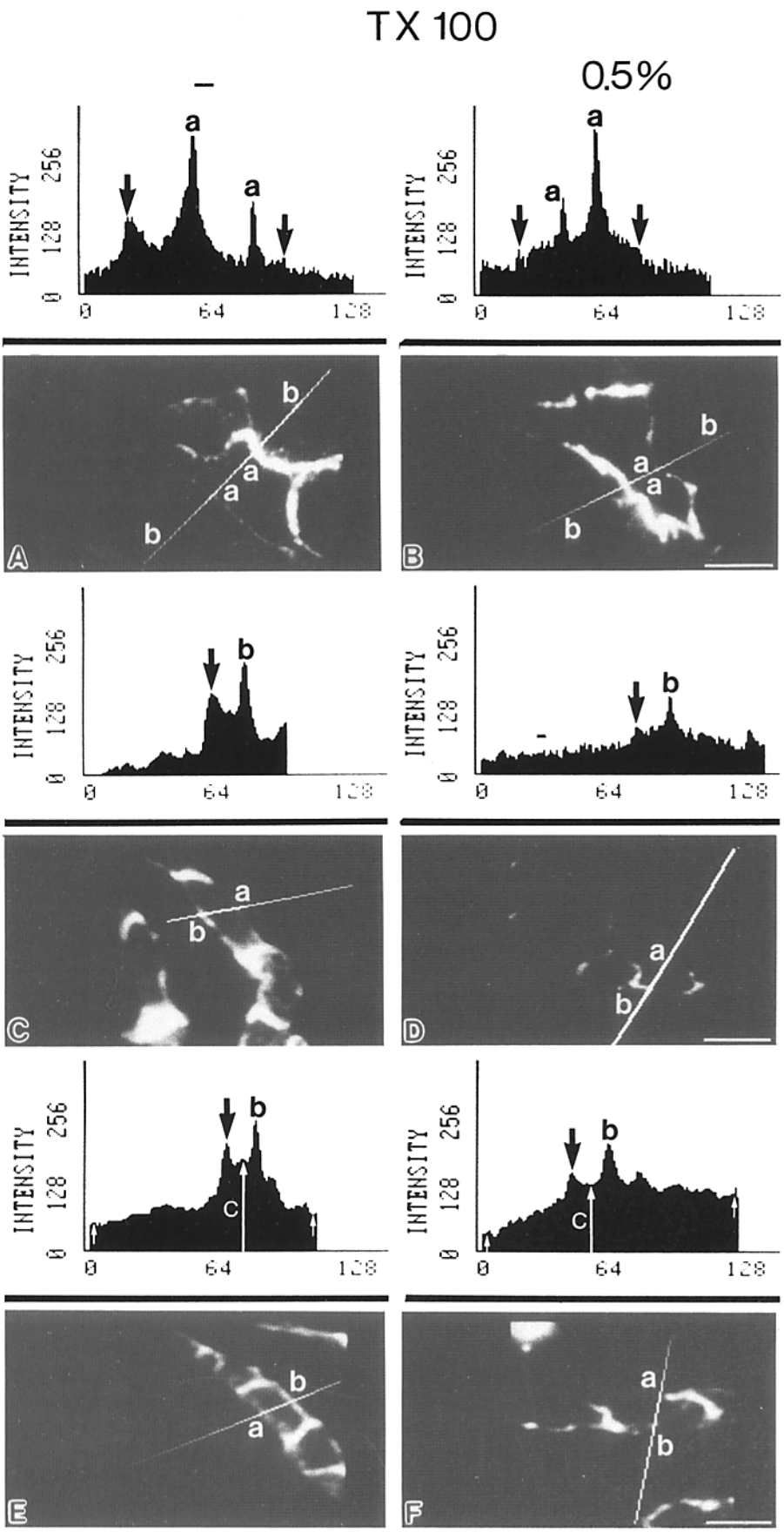

Figure 4. Immunofluorescence localization and measurement by digitized video analysis of MDCK cell membrane proteins in semi-thin frozen sections after TX-100 extraction. MDCK cells were incubated, extracted in TX-100 (*B*, *D*, and *F*) and processed as described in Fig. 3. The fluorescence images were captured with a silicon-intensified video camera directly from the fluorescence microscope, digitized, and stored on the hard disk. Each section shows the digitized image (*lower half*) and the corresponding fluorescence profile along the line (*upper half*) in pixel units (0–255). In the profiles, *a* and *b* show the position of apical and basal membranes. The black arrowheads point the fluorescence peak in the incorrect domain (i.e., the basal fluorescence of a mostly apical marker). (*A*) A1 MAb, unextracted. (*B*) A1 MAb, preextracted in TX-100. Note that *A* and *B* show folds of the monolayer with the apical domains of two adjacent areas facing each other. (*C*) B1 MAb, unextracted. (*D*) B1, preextracted in TX-100. (*E*) B2 MAb, unextracted. (*F*) B2, preextracted. Small white arrows in *E* and *F* show extracellular fluorescence (background). Large white arrow (*c*) shows cytoplasmic fluorescence. Bars: (*A* and *B*) 18 μm; (*C*, *D*, *E*, and *F*) 21 μm.

was measured within the cell (Fig. 4, *E* and *F, central white arrows, c*). Cytoplasmic fluorescence was 6–40 pixel units higher than the extracellular background. This relatively small fluorescence was very extractable in TX-100 (Table II, *Cytoplasm*). For A1, B1, and B2, the fluorescence on the plasma membrane was higher than the cytoplasmic fluorescence ("peaks"), even in the case of the smaller peaks, namely those in the incorrect domain from detergent extracted cells. Therefore, even these smaller peaks could be measured with no uncertainty. This was not the case for B2-m. For this marker, only the lateral domain showed clear peaks above the cytoplasmic fluorescence. The fluorescence profile did not show any apical or basal peak in nearly 60% of the cells. In those cases, the values were taken from the pixels on the corresponding domain as judged by parallel phase images. These values (apical and basal for B2-m) may contain a larger error due to the cytoplasmic fluorescence. The corresponding extractabilities are shown in Table II for comparison with the much lower extractability in the lateral domain. To determine the possible contribution of cytoplasmic fluorescence, a parallel set of extractability values was obtained for all the markers by subtracting cytoplasmic fluorescence from peak values (Table II, *C*). Since extracellular background was not decreased by detergent extraction we considered *E* values as unbiased and will use them hereafter.

While only 6% of A1 was extracted from the apical surface, >70% was extracted from the basal and lateral membrane domains (Table II, *E*). Conversely, B1 and B2 showed small apical (incorrect domain) fluorescence peaks in unextracted cells (Fig. 4, *C* and *E*), which were decreased in size, although not completely abolished, by TX-100 (Fig. 4, *D* and *F*). Levels of B1 and B2 extractability were ~50% in the apical surface and ~16% in the lateral surface (Table II, *E*). The other basolateral marker, B2-m, exhibited a similar pattern of extraction; like B2, it showed intermediate levels of extraction from the basal surface; like B1 and B2, the maximum insolubility in TX-100 was observed on the lateral surface.

Since the A1 mAb binding site might involve a carbohydrate epitope (Table I) it was conceivable that the extractable fraction of A1 was composed of glycolipids carrying the same epitope as the 215-kD antigen. This possibility was ruled out by the following experiment: MDCK cell monolayers were grown on glass coverslips for 1 d and fixed in either 2% PFA at 4°C or 96% methanol at −20°C. Some coverslips were further extracted in chloroform/methanol 2:1. The latter extraction did not result in significant decrease of A1 binding in any case as determined by indirect RIA.

Basolateral Antigens Are Fully Extractable by TX-100 in Cells Prevented from Establishing Cell–Cell Contacts

Previous work has shown that incubation in low calcium

Table II. Differential Extractability in TX-100 of MDCK Cell Membrane Antigens from the Apical, Lateral, and Basal Domains of the Plasma Membrane

		Extractable fraction (in percent)				
Probe	BKG	Apical	Lateral	Basal	Cytoplasm	*n*
1 d						
A1	E	6 ± 30*	70 ± 10	76 ± 11	98 ± 24	5
	C	10 ± 14*	85 ± 7	95 ± 4		
B1	E	50 ± 29*	17 ± 12	16 ± 12	83 ± 12	3
	C	93 ± 11*	27 ± 8	27 ± 7		
B2	E	55 ± 13*	14 ± 6	34 ± 23	90 ± 12	4
	C	64 ± 7*	20 ± 4	38 ± 15		
B2-m	E	66 ± 16*	4 ± 19	48 ± 30*	44 ± 18	5
	C	81 ± 14*	6 ± 15	58 ± 27*		
4 d						
A1	E	7 ± 10*	70 ± 7	76 ± 8	92 ± 18	3
	C	14 ± 9*	83 ± 3	91 ± 3*		
B1	E	55 ± 3*	24 ± 16	23 ± 17	85 ± 30	3
	C	84 ± 12*	26 ± 10	27 ± 16		
B2	E	60 ± 28	23 ± 18	45 ± 16	72 ± 18	3
	C	88 ± 16*	27 ± 15	53 ± 14		
B2-m		ND				

MDCK monolayers were plated at immediate confluency and incubated for 1 or 4 d in D-MEM. After fixation the cells were frozen sectioned taking care that the thickness was similar in all sections. The sections were incubated first with the mAb or B2-m and then with rhodamine-coupled affinity-purified goat anti-mouse IgG. For each marker the gain of the video camera was set so that the fluorescence from nonextracted cells fell in the upper part of the linear range. The images from TX-100-extracted cells were acquired using the same gain. To compensate differences in section thickness, images from 18 to 30 cells in separate sections were used for both extracted and nonextracted conditions, and the fluorescence was averaged for each lot. The extractable fraction was obtained as the ratios between the averages of extracted/nonextracted fluorescence intensity (peak height after subtracting either extracellular fluorescence *E* [see Fig. 4, *E* and *F, small white arrows*] or cytoplasmic fluorescence *C* [see Fig. 4, *E* and *F, central white arrow*]) from *n* groups of six cells (three profiles per cell) for each plasma membrane domain. The data are presented as mean ± SD.

* The difference between means ($X - X_{lateral}$) is statistically significant by *t* test, $p < 0.05$. The test was not applied to cytoplasmic extractabilities. The 100% represents the average fluorescence for each domain in nonextracted cells. Therefore the percents of extractability in different domains cannot be added.

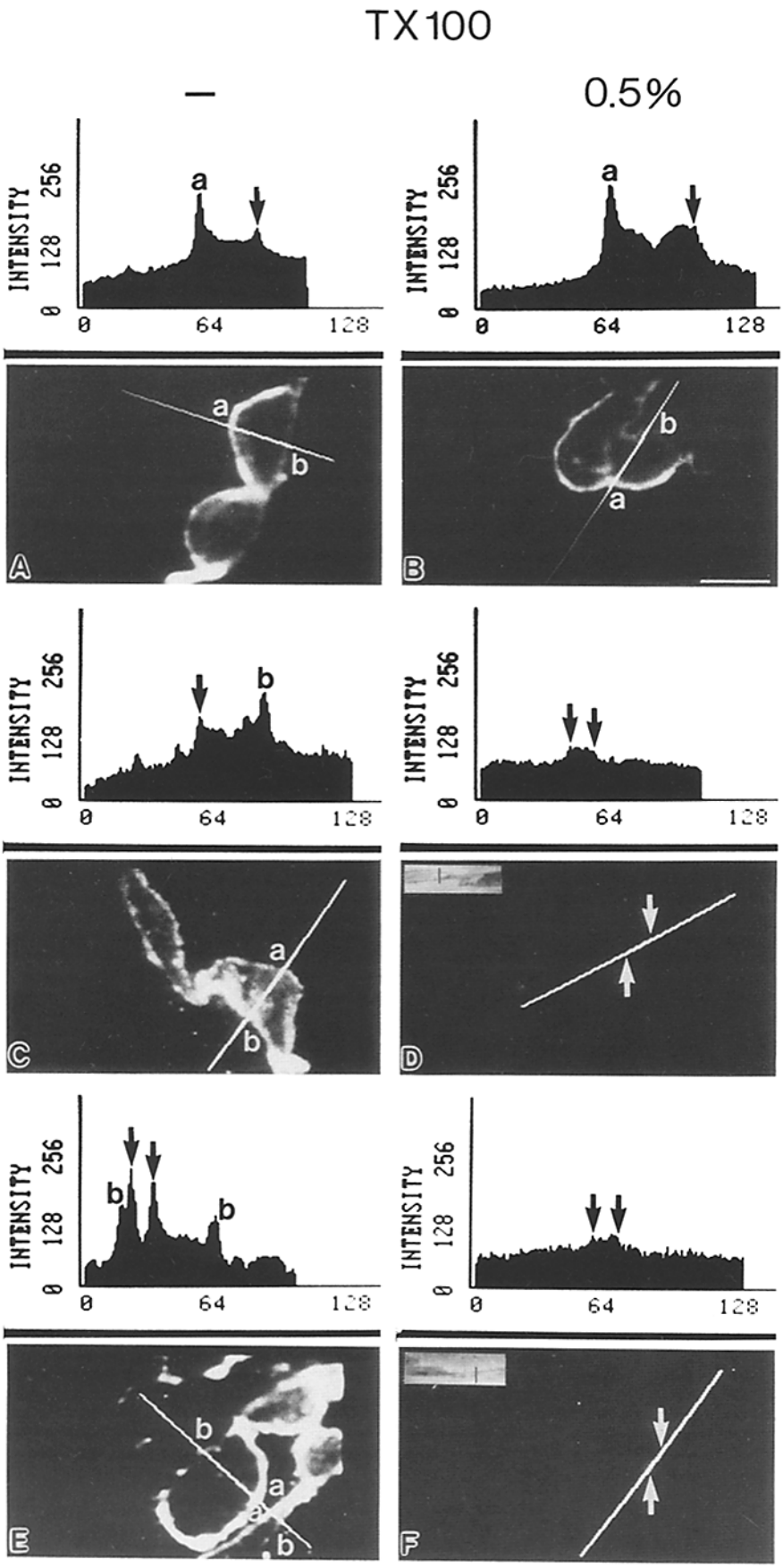

Figure 5. Immunofluorescence localization and measurement by digitized video analysis of membrane proteins in semithin frozen sections of MDCK cells kept in low calcium medium. MDCK cells were plated at immediate confluency and, after 2 h, the medium was replaced with serum-free S-MEM (~5 μM calcium). After 24 h some monolayers were extracted in 0.5% TX-100 and all the monolayers were fixed and processed as described in Fig. 4. (*A*) A1 MAb, unextracted. (*B*) A1 MAb, preextracted in TX-100. (*C*) B1 MAb, unextracted. (*D*) B1, preextracted in TX-100. (*E*) B2 MAb, unextracted. Note that *E* shows a fold of the monolayer with the apical domains of two adjacent areas facing each other. (*F*) B2, preextracted. Note that both basolateral markers are not polarized and are very extractable in TX-100. White arrows in *D* and *F* show position of the plasma membrane on the profile line. (*Inset*) Corresponding phase image. Bar, 19 μm.

medium (~5 μM) prevents MDCK cells from forming complete cell-cell contacts (27). Under these conditions A2 antigen (184 kD) was found completely polarized, while B1 (63 kD) was not (82), and only very discontinuous tight junctional structures can be observed by ZO-1 monoclonal antibody fluorescence (76, 84). In this work, those observations were confirmed and extended to two more membrane proteins: A1 was polarized in low calcium medium (Fig. 5 *A*) while B2 was not (Fig. 5 *E*).

Strikingly, both basolateral markers were almost totally extracted in 0.5% Triton X-100 from monolayers developed in low calcium medium. Only a small plateau of cytoplasmic fluorescence was left after detergent extraction (Fig. 5, *D* and *F*). This result was independently confirmed by RIA (not shown). On the other hand, the apical antigen A1 was resistant to TX-100 extraction in low calcium medium, and was preferentially removed from the basal (attached) surface (Fig. 5 *B*). Thus, the cytoskeletal linkage of A1 is not dependent on the establishment of normal cell-cell contacts, as is the case with the basolateral antigens B1 and B2.

Recently, Nelson and Veshnock (48, 49) have shown that the development of an insoluble fodrin network on the basolateral membrane correlates with the polarization of the basolateral marker Na^+-K^+ ATPase which forms a stable complex with ankyrin and fodrin (50). We found that destabilization of this network by 4 mM DTT significantly facilitated extraction of B1, but not A1 (Table III). Thus, this result and the detergent extractability of B1 and B2 in cells prevented from forming cell-cell contacts, are compatible with a basolateral fodrin cytoskeleton (4, 73) anchoring B1 but not A1.

Table III. Extraction of the TX-100-insoluble Fraction of MDCK Cell Plasma Membrane Proteins from the Cytoskeletal Preparations

Extraction medium	mAb	Pellet associated protein (in percent)
None (control)	A1	100
	B1	100
4 mM diamide, →6 M urea	A1	87 ± 3
	B1	100 ± 9
4 mM DTT, →6 M urea	A1	99 ± 10
	B1	43 ± 5*

MDCK cell monolayers were extracted with 0.5% TX-100 in EB. The remaining cytoskeletal preparations were then treated with 0.1 mg/ml DNAase I for 1 h in PBS supplemented with 1 mM Mg^{++} and 2 mM EGTA. The cytoskeletons were scraped with a rubber policeman in PBS, 1 mM EDTA, 0.5% TX-100, and homogenized with a glass homogenizer (Dounce; 50 strokes in the same buffer). The homogenates were supplemented with a concentrated stock solution of either diamide or DTT up to the final concentrations shown in the table for 30 min at room temperature. Urea was added as powder up to a final concentration of 6 M. The homogenates were spun at 215,000 *g* for 30 min at 10°C, the pellets were washed in PBS, and processed for indirect RIA. The control values (100%: 10,963 ± 2,775 cpm for A1, and 12,533 ± 4,465 cpm for B1) were obtained from untreated homogenates. The data are presented as mean ± SD from three independent experiments.

* A significant difference of means as compared with control values (*t* test, $p < 0.05$).

Immobile Fractions of Basolateral Antigens Are Larger in the Basolateral Domain than in the Apical Domain

FRAP reports on the diffusion coefficient, D, of a labeled molecule of interest, on the fraction of label in a region of the cell that can diffuse at all, and on the fraction of cells in a population in which no diffusion can be measured (hereafter referred to as totally immobile fraction [TIF]). We used FRAP to determine all of these parameters for fluorescent Fab fragments of A2 and B1 mAbs. We also labeled the class I major histocompatibility complex antigens, DLA, with fluorescent B2-m, a low molecular mass (~12 kD) monovalent probe. No active Fab fragments of A1 mAb (an IgM) or B2 mAb could be obtained. The measurements were carried out on MDCK monolayers grown on nylon filter chambers similar to those described by Cereijido et al. (12), except that the filters were covered by native, instead of fixed, collagen. Fluorescent Fab fragments or B2-m were added to either the apical or the basal side of the monolayers to study the mobility of the antigen in the apical and in the basolateral membrane. Comparative measurements of A2 in both membranes were, unfortunately, not possible, because this antigen is so intensely polarized that no specific signal can be detected on the basal membrane. The results are shown in Table IV.

The (geometric) mean diffusion coefficients, D, for all labels applied to the apical surface were in the range 1.1–1.3 $\times 10^{-9}$ cm^2/s^{-1}. None differed significantly from any other. Similar D's were measured on the free surface of sparse cells (unpolarized for basolateral antigens). Diffusion coefficients for labels on the basal surface of confluent monolayers were ~50% smaller, in the range 0.6–0.9 $\times 10^{-9}$ cm^2/s^{-1}, but the difference was not statistically significant (Table IV).

The mobile fraction, R, of diffusing molecules was estimated from the extent of recovery of fluorescence after photobleaching. The apparent R were between 38 and 65%. These values were an underestimate of the recovery of fluorescence, since the fluorescence from labeled cells was 1.5–3.5 times the fluorescence from cell blanks (either unlabeled or treated with only the second Fab). The endogenous fluorescence from cell blanks did bleach but did not recover. Hence, we can make a better approximation to the actual fraction of mobile labels by correcting the apparent R for a significant fraction of fluorescence that was immobile. These corrected values, from experiments in which sufficient (6–12) blanks were measured to give a reliable estimate, were in the range of 64–84% (Table IV). They are high but do not reach 90–100%. No difference in R was observed between the apical and the basal surface, for all antigens studied. As shown in a previous work (86), R did not correlate with TX-100 extractability. The overall conclusion from measurements where recovery was observed is compatible with large mobile fractions behaving similarly in the apical or basolateral domains.

D and R can only be determined if some recovery is found after photobleaching. In our experiments, we found a large percent of measurements in which no recovery of fluorescence at all could be measured (TIF), even though the cells appeared to be labeled to the same extent and in the same way (uniform faint fluorescence, rather than the coarse speckles indicating aggregation of label) as cells in which recovery of fluorescence was found. Since 100% of the cells have B1 epitopes, lack of recovery cannot be attributed to unspecific fluorescence in antigen negative cells. TIF did not correlate with time after labeling (not shown) and were similar at 10°C, therefore, TIF cannot be attributed to endocytosed antigen. Experience with FRAP in fibroblasts indicates

Table IV. FRAP Determinations of Monovalent Probes for MDCK Plasma Membrane Proteins

Domain	Probe	TIF (in percent)	R (in percent)	D	TX-100-insoluble*	n
				$10^{-9}cm^2s^{-1}$		
Apical (confluent)	A2 Fab	0	84 ± 16	1.1	<10	16
Apical (sparse)	B1 Fab	0	70 ± 14	1.2	<10	7
	B2-m	8	72 ± 16	1.3	ND	24
Basal (confluent)	B1 Fab	28	64 ± 10	0.6	84	16
	B2-m	52	65 ± 8	0.9	42	25

Sparse MDCK cells were grown for ~24 h on glass coverslips. Confluent MDCK cells were grown for the same period on nylon filters coated with native collagen gels separating two chambers. For this condition the probes were added from the medium and there was little or no diffusion to the basal side. The laser beam was focused to the apical domain. For the confluent condition, the probes were added from either the apical or basal chamber. TIF is the percent of measurements (cells) that showed <15% recovery (*R*). *D* and *R* are, respectively, the geometric diffusion coefficient and percent of recovery calculated from measurements with $R > 15\%$. *R* is shown as average (corrected for nonrecoverable background) ± SD. The 95% confidence intervals for *D* were 0.6 × mean and 2.0 × mean.

* TX-100-insoluble fractions are values from Table II (Basal B1 and B2-m) and separate video analysis determinations for B1 and A2 (*apical*) extractability on semi-thin frozen sections (not shown). *n* is the number of measurements (cells).

that it reflects variation between cells (86), but in a confluent epithelial monolayer we cannot discriminate whether neighboring spots would reflect conditions in the same cell or in closely adjacent cells, specially for the basolateral domain where interdigitations are frequently observed. Hence, we do not have direct evidence in this system on whether TIF reports on heterogeneity in the cell population or microheterogeneity in the mobility of the proteins within the membrane surface of a given cell.

A2 fluorescence recovered in all cells labeled with Fab (TIF = 0; Table IV). On the other hand, B1 and B2-m showed 28 and 52% of the cells, respectively, failing to recover any fluorescence at all on the basolateral membrane. Corresponding TIF values on the apical membrane were significantly lower (0–8%; Table IV). Therefore, when FRAP is measured with monovalent probes, TIF correlates roughly with the TX-100 insolubility of A2, B1, and B2-m from the basal, lateral, and apical domains (Tables II and IV). Altogether, these data are compatible with a model consisting of (*a*) highly mobile fractions for all the antigens, the size of which does not correlate with the degree of polarity, and (*b*) domain specific cytoskeleton anchored fractions for B1, B2, B2-m, and A1, but not for A2.

Discussion

Four MDCK Plasma Membrane Proteins Are Selectively Unextractable in a Domain-specific Fashion

Previous work with epithelial cells in culture had shown that lectin receptors (17) might be significantly immobilized. The results of this report indicate the existence of domain specific cytoskeletal anchorage of one apical (A1) and three basolateral (B1, B2, and class I major histocompatibility antigens) integral plasma membrane proteins of MDCK cells. Extraction of MDCK cells with Triton X-100 under conditions that preserve the cell membrane skeleton detects two populations of these markers: an insoluble one, largely concentrated in the correct domain, and a soluble one, that accounts for most of the antigen found in the incorrect domain.

The Singer and Nicholson model (71) clearly predicts the solubilization of integral membrane proteins in detergents. The lack of solubility, on the other hand, has been explained by cytoskeletal associations in the case of band 3/ankyrin/spectrin (67), T-lymphoma gp180 glycoprotein/fodrin (8), the heparan sulfate proteoglycan in Schwann cells (11), and the 100-kD/actin in the microvillus (31, 43). Since fodrin is present in the submembrane cytoskeleton of the basolateral domain (48), some components of the microvillar system are present in kidney epithelia (59) and actin is present in the microvilli of MDCK cells (Fig. 1); cytoskeletal associations similar to those cited above may result in the insolubility of A1, B1, and B2 in TX-100. On the other hand, insolubility in TX-100 might not equate with association of membrane proteins to the cytoskeleton and may be generally reporting on immobilization of the proteins to other insoluble molecules as those composing the glycocalyx, the extracellular matrix, or simply to other membrane proteins indirectly anchored by the cytoskeletal scaffold after detergent extraction.

Each membrane antigen studied here showed a characteristic Triton X-100-insoluble fraction. This fraction was largely dependent on the existence of cell–cell contacts for B1 and B2: both antigens were totally extractable in cells with incomplete cell–cell contacts. Nelson and Veshnock (48) have recently reported that the development of an insoluble network of fodrin in the basolateral membrane is dependent on the establishment of cell–cell contacts and therefore can be blocked by incubation in 5 μM Ca^{++}. They have also presented evidence for a specific interaction between a basolateral marker of MDCK cells, Na^+–K^+ ATPase, and ankyrin (50), a protein known to form complexes with spectrin in the red cell (5, 9). In this work, we have shown that the extractability of B1 and B2 is modified by conditions that affect the stability of the fodrin network (Table III). Thus, in combination with Nelson and Veshnock's results, our data suggest that the polarization of several basolateral markers is linked to the formation of a basolateral fodrin network, with which they appear to interact. Whether this interaction is direct, through the cytoplasmic domain of the basolateral proteins, or indirect, via an intermediate membrane protein, is still open to study. Because insoluble fodrin is much more stable (49), linkage to this network may result in a prolonged half-life for the membrane proteins that would contribute to their relative polarization to the basolateral membrane.

From the two apical markers studied, one (A1) behaved like the basolateral markers in that it displayed large unextractable fractions in the correct (apical) membrane and was almost completely extractable from the incorrect (basolateral) membrane. A main difference with the basal antigens, however, was that the insoluble pool of A1 did not show any dependence on cell–cell contacts. The nature of the apical membrane–specific cytoskeletal structures that bind A1 is still unclear; it may be speculated that they form part of the terminal web or the microvillar core structures (46). The second apical marker, A2, was completely extractable

under the conditions used in this work. Strikingly, it was also the most stringently polarized and it shared with A1 the ability to polarize in low calcium medium (although A1 is less polarized than A2), in clear contradistinction with the basolateral markers B1 and B2 (Fig. 5; see also reference 82). With these data, we cannot exclude the possibility that A2 is anchored via a "labile" cytoskeletal anchorage that may be broken under our experimental manipulations. On the other hand, the maintenance of A2 polarization may be dependent on a fence mechanism different from the tight junction, or on some other restriction mechanism, perhaps complex aggregation or active exclusion from the basolateral domain. We have calculated that even high aggregation numbers would have a low effect on D (Edidin, unpublished observations). Aggregation of membrane proteins might be a significant factor if "filter"-like fences existed in the bilayer. Such a structure, perhaps incomplete tight junctional elements, might permit the passage of single molecules (as would be the case for the mobile fraction of A1), but restrict the diffusion of aggregates (as in the case of fully polarized antigens like A2). Some indirect evidence suggests that filters may be operational even in confluent monolayers: A2 is partially excluded from the boundaries of the apical domain (83, 84), while A1 is not. If patching of A1 is induced by addition of a second complete antibody on living cells, on the other hand, the patches are excluded from the same boundary area (Salas, P. J. I., unpublished observations). Such an incomplete fence or filter may be present in cells that lack complete tight junctions.

Finally, the possibility should be considered that some of the cytoskeletal interactions described here may be covalent. Transglutaminase has been shown to cause cross-linking of erythrocyte proteins with the cytoskeleton, although at nonphysiologically high Ca^{++} levels (38, 69). The presence of EGTA in our extraction buffer rules out an artifact caused by this mechanism. However, in rat hepatocytes, transglutaminase activity is found associated with a large molecular weight substrate comprising the lateral plasma membrane domain (72, 80), which suggests a possible physiological role for this enzyme in cross-linking surface and cytoskeletal components. The resistance of A1 and B1 cytoskeletal complexes to urea extraction (Table III) suggests the possibility of covalent linkage.

Correlation between TIF and Detergent-unextractable Fractions of Basolateral Antigens

We studied by FRAP the diffusional parameters of antigens localized in the apical and basolateral membrane. The probes were added differentially to both domains in cells grown on collagen-coated nylon nets, similar to those originally used by Cereijido et al. (12), except that in our case the collagen gels were native to allow diffusion of antibodies. We could use only three monovalent probes in FRAP measurements: B1 Fab, B2-m, and A2 Fab. A2 is a highly polarized antigen (polarity ratio >15:1; reference 82), so no signal could be detected on the basolateral domain. B1 and B2-m appear in the apical domain in large amounts when the cells are prevented from forming cell–cell contacts (either in sparse cells or in cells incubated in low calcium medium). Upon establishment of a confluent monolayer, B1 (82) and B2 (unpublished observations) become polarized over a 4-d period. Significant amounts of B1 and B2 are still present in the apical (incorrect) domain 24 h after plating and are amenable for FRAP measurements, while A2 is already polarized and cannot be detected in the basolateral (incorrect) domain. In the 4-d stage, on the other hand, only tracer amounts of B1 and B2 are present in the apical domain. These amounts could be determined as small peaks above background in the fluorescence profiles on semi-thin frozen sections, but we could not discriminate them from cellular autofluorescence in intact cells. Therefore FRAP could be measured in the incorrect domain only when significant amounts of the antigen were present. Under these technical restrictions, we found small differences in the diffusion coefficients and no differences in the recovery fractions between apical and basolateral membranes for both basolateral markers. The values of these parameters reported here for B1 and B2-m are in good agreement with similar values reported by Jesaitis and Yguerabide (34) for $(Na^+–K^+)$ ATPase on the free surface of subconfluent MDCK cells and in scraped confluent monolayers. The latter condition has been extensively used to load macromolecules in various cell types and is likely to increase cytoplasmic calcium levels that may affect the cytoskeletal functions. This basolateral marker of MDCK cells shows similar kinetics of polarization and similar dependence on intercellular contacts as our B1 and B2 markers (48, 74).

If molecules anchored to the cytoskeleton are resistant to extraction by detergent, then we might expect the fraction of extractable molecules to correlate well with the fraction of molecules mobile in FRAP measurements on single cells. In fact, resistance to extraction correlates with the incidence of cells in which little or no recovery of fluorescence could be observed after photobleaching, the TIF of the population examined. This correlation is in fact likely to reflect the mobile fraction of labeled molecules on each cell. If the values for detergent extractability and, by extension, mobile fraction are normally distributed, then we expect a large fraction of cells to have a lower extractability than average. These cells would not show detectable mobility of labeled membrane proteins in a FRAP experiment. For example, 48 ± 30% of B2-m is extractable from the basal domain of cells plated at confluency for 24 h. With this standard deviation, 16% of cells must have <18% extractable, and if this correlates with mobility, these cells would certainly be scored in the TIF. No cells had TIF for A2, which was completely extracted by TX-100. On the other hand, 30–52% of the cells showed TIF for B1 and B2-m in the basolateral membrane (where they are poorly extractable), while only 0–8% showed TIF on the apical membrane (where their extractability is higher). Like the extraction experiments, the FRAP data are consistent with the existence of domain-specific interactions of basolateral antigens with the submembrane cytoskeleton, and mobile fractions present in both apical and basolateral domains.

These domain-specific phenomena are reminiscent of the lectin- or substrate-induced modulation of lateral diffusion reported for nonpolarized cells (20), so-called "global modulation". Such modulation of mobility was also observed for molecules of N-CAM upon differentiation of neuroblastoma cells (57). We were not able to find differences in total cellular TX-100-extractable fractions of four membrane antigens between 1- and 4-d confluent monolayers. Nonetheless, two

of them are more polarized in the latter stage. These determinations may be partially masked by an intracellular pool of membrane antigens, presumably TX-100 soluble. However, they support the notion that there is a mobile and TX-100-soluble fraction of these antigens even in the fully polarized stage. We speculate that this fraction may be important for turnover of plasma membrane proteins.

Using FRAP, it has been shown that Band III is considerably restricted in its ability to diffuse in the plane of the membrane. The restriction depends on interactions with the ankyrin spectrin submembrane cytoskeleton, since the diffusion coefficient, very low in normal erythrocytes ($D = 4.5 \times 10^{-11}$) is increased 50-fold in spectrin-deficient spherocytes (68) and under conditions that favor spectrin dissociation (79). The interaction between a subpopulation (~40%) of Band III molecules and spectrin is mediated by ankyrin (5), while another subpopulation shows free rotational diffusion (13, 51), and seems to be confined within the spaces defined by the submembrane spectrin network (36, 79). It is not known whether the basolateral fodrin cytoskeleton forms a network in epithelial cells. However, if the epithelial spectrin was organized like its erythroid counterpart, it could be predicted that basolateral membrane proteins should have a detergent-extractable and -diffusible fraction as well as a cytoskeleton-anchored fraction. In that case the high D's that we measured in FRAP experiments are compatible with a coarse or incomplete fodrin network with free diffusion spaces in the order of the size of our laser spot (~1 μm). In this model, TIF would correspond either to cells with a denser network or to spots located on nodes of the network. On the other hand, it has been shown that the Na^+-K^+ ATPase/ankyrin/spectrin complex can be formed in vitro, with molecules in solution (50). Therefore, we cannot rule out the possibility that freely diffusive plasma membrane proteins located within the spaces of the fodrin network may bind to ankyrin/spectrin sites during the course of the Triton X-100 extraction. In that case, the detergent insolubility may be reporting more on the number of binding sites available than on the number of molecules bound to the cytoskeleton at any given time. Even under this model that explains FRAP and detergent extraction together, the data presented in this work indicates that epithelial cells have a specialized submembrane cytoskeleton capable of immobilizing subpopulations of plasma membrane proteins in a domain-specific fashion.

Recent work has shown that signals for the retention of proteins in the ER may be localized in either luminal (47) or cytoplasmic (53) domains (see reference 62 for a review). Plasma membrane proteins lacking these signals would be carried by bulk flow to the Golgi apparatus and then to the cell surface. With the exception of Band III, there is no evidence for the localization of retention signals in plasma membrane proteins. It has recently been reported that major histocompatibility antigens or epidermal growth factor with truncated tails do not show increased lateral diffusion (23, 37). A similar result has been reported for vesicular stomatitis virus (VSV) G glycoprotein (66), suggesting the possibility that protein–protein interactions at the ectoplasmic domain may result in restrictions to lateral mobility of membrane proteins.

Domain-specific Anchoring to the Submembrane Cytoskeleton and Epithelial Polarity

Previous work has shown that epithelial surface polarity in MDCK cells is generated by intracellular sorting and vectorial delivery of apical and basal proteins (10, 41, 45, 55, 58, 64). The fence role of tight junctions has been often stressed (17, 34, 81). This report highlights the necessity of tight junctions to keep mobile fractions segregated and also the important contribution of intradomain restrictions to the lateral mobility for four of the five probes tested. These restrictions may be particularly effective by preventing recycling of the protein and, thus, its exposure to the lysosomal environment and degradation. Matlin and Simons (41) and Pesonen and Simons (54) have shown that VSV G protein incorporated via virus fusion to the apical surface is partially degraded and partially transcytosed to the basolateral membrane, its normal target membrane in MDCK cells infected with VSV. It is a clear prediction of the work in this report that the half-life of anchored antigens will be increased as opposed to antigens in the incorrect surface. It is also expected that recycling receptors with very low fractions in the cell surface and large intracellular pools will not be anchored in significant amounts to the cytoskeleton.

It is a pleasure to thank Drs. Frederick Maxfield (Columbia University), Joel Pardee (Cornell University Medical College), and Walter Stuhmer (Max Planck Institut fur Biophysikalische Chemie, FRG) for critical discussion and suggestions; and Mr. James Denis for electron microscopy.

This work was supported by research grants from the National Institutes of Health (GM-34107 to E. Rodriguez-Boulan and AI-14584 to M. Edidin), National Science Foundation (DCB-8442489 and INT-841440), American Heart Association, New York Branch, by an established investigator award to Dr. E. Rodriguez-Boulan. Dr. P. Salas was recipient of awards from CONICET and Fundacion A. J. Roemmers (Argentina). Drs. P. Salas and D. E. Vega-Salas are Career Investigators at CONICET. J. Hochman was recipient of a Damon Runyon/Walter Winchell fellowship.

The authors dedicate this work to the memory of the admired scientist and teacher, Dr. Eduardo P. De Robertis, who passed away on May 30, 1988.

Received for publication 28 December 1987, and in revised form 28 July 1988.

References

1. Almers, W., and C. Stirling. 1984. Distribution of transport proteins over animal cell membranes. *J. Membr. Biol.* 77:169–186.
2. Almers, W., P. R. Stanfield, and W. Stuhmer. 1983. Lateral distribution of sodium and potassium channels in frog skeletal muscle: measurements with a patch clamp technique. *J. Physiol. (Lond.).* 336:261–284.
3. Apgar, J. R., and M. F. Mescher. 1986. Agorins: major structural proteins of the plasma membrane skeleton of P815 tumor cells. *J. Cell Biol.* 103: 351–360.
4. Becker, P. S., C. M. Cohen, and S. E. Lux. 1986. The effect of mild diamide oxidation on the structure and function of human erythrocyte spectrin. *J. Biol. Chem.* 261:4620–4628.
5. Bennet, V. 1982. The molecular basis for membrane: cytoskeleton association in human erythrocytes. *J. Cell. Biochem.* 18:49–65.
6. Ben-Ze'ev, A., A. Duerr, F. Solomon, and S. Penman. 1979. The outer boundary of the cytoskeleton: a lamina derived from plasma membrane proteins. *Cell.* 17:859–865.
7. Bordier, C. 1981. Phase separation of integral membrane proteins in Triton X-114 solution. *J. Biol. Chem.* 256:1604–1607.
8. Bourguignon, L. Y. W., S. J. Suchard, N. L. Nagpal, and J. R. Glenney, Jr. 1985. A T-lymphoma transmembane glycoprotein (gp180) is linked to the cytoskeletal protein, fodrin. *J. Cell Biol.* 101:477–487.
9. Branton, D., C. M. Cohen, and J. Tyler. 1981. Interaction of cytoskeletal proteins on the human erythrocyte membrane. *Cell.* 24:24–32.
10. Caplan, M. J., H. C. Anderson, G. E. Palade, and J. D. Jamieson. 1986. Intracellular sorting and polarized cell surface delivery of (Na^+-K^+)-ATPase, an endogenous component of MDCK cell basolateral plasma membranes. *Cell.* 24:24–32.
11. Carey, D. J., and M. S. Todd. 1986. A cytoskeleton-associated plasma membrane heparan sulfate proteoglycan in Schwann cells. *J. Biol. Chem.* 261:7518–7525.
12. Cereijido, M., E. S. Robbins, W. J. Dolan, C. A. Rotuno, and D. D. Sabatini. 1978. Polarized monolayers formed by epithelial cells on a permeable and translucent support. *J. Cell Biol.* 77:853–880.

13. Cherry, R. J. 1979. Rotational and lateral diffusion of membrane proteins. *Biochim. Biophys. Acta.* 559:289–327.
14. Clemetson, K. J., D. Bienz, M. L. Zahno, and E. F. Luscher. 1984. Distribution of platelet glycoproteins and phosphoproteins in hydrophobic and hydrophilic phases in Triton X-114 phase partition. *Biochim. Biophys. Acta.* 778:463–469.
15. Cutler, D. F., P. Melancon, and H. Garoff. 1986. Mutants of the membrane-binding region of Semliki Forest virus E2 protein. II. Topology and membrane binding. *J. Cell Biol.* 102:902–910.
16. Diamond, J. M. 1977. The epithelial junction: bridge, gate, and fence. *Physiologist.* 20:10–18.
17. Dragsten, P. R., J. S. Handler, and R. Blumenthal. 1982. Fluorescent membrane probes and the mechanism of maintenance of cellular asymmetry in epithelia. *Fed. Proc.* 41:48–53.
18. Drenckhahn, D., and H. Franz. 1986. Identification of actin, alpha-actinin, and vinculin-containing plaques at the lateral membrane of epithelial cells. *J. Cell Biol.* 102:1843–1852.
19. Drenckhahn, D., K. Schluter, D. P. Allen, and V. Bennett. 1985. Colocalization of band 3 with ankyrin and spectrin at the basal membrane of intercalated cells in the rat kidney. *Science (Wash.).* 230:1287–1289.
20. Edelman, G. M. 1976. Surface modulation in cell recognition and growth. *Science (Wash.).* 192:218–226.
21. Edelman, G. M. 1986. Cell adhesion molecules in the regulation of animal form and tissue pattern. *Annu. Rev. Cell Biol.* 2:81–116.
22. Edidin, M., and T. Wei. 1982. Lateral diffusion of H-2 antigens on mouse fibroblasts. *J. Cell Biol.* 95:458–462.
23. Edidin, M., and M. Zuniga. 1984. Lateral diffusion of wild-type and mutant Ld antigens in L cells. *J. Cell Biol.* 99:2333–2335.
24. Elsdale, T., and J. Bard. 1972. Collagen substrata for studies on cell behavior. *J. Cell Biol.* 54:626–637.
25. Fey, E. G., K. M. Wan, and S. Penman. 1984. Epithelial cytoskeletal framework and nuclear matrix-intermediate filament scaffold: three-dimensional organization and protein composition. *J. Cell Biol.* 98:1973–1984.
26. Fujiki, Y., A. L. Hubbard, S. Fowler, and P. B. Lazarow. 1982. Isolation of intracellular membranes by means of sodium carbonate treatment: application to endoplasmic reticulum. *J. Cell Biol.* 93:97–102.
27. Gonzalez-Mariscal, L., B. Chavez de Ramirez, and M. Cereijido. 1985. Tight-junction formation in cultured epithelial cells (MDCK). *J. Membr. Biol.* 86:113–125.
28. Gumbiner, B., and K. Simons. 1986. A functional assay for proteins involved in establishing an epithelial occluding barrier: identification of an uvomorulin-like polypeptide. *J. Cell Biol.* 102:457–468.
29. Herzlinger, D. A., and G. Ojakian. 1984. Studies on the development and maintenance of epithelial cell surface polarity with monoclonal antibodies. *J. Cell Biol.* 98:1777–1787.
30. Hochman, J. H., Y. Shimizu, R. DeMars, and M. Edidin. 1988. Specific associations of fluorescent b-2-microglobulin with cell surfaces. The affinity of different H-2 and HLA antigens for b-2-microglobulin. *J. Immunol.* 140:2322–2329.
31. Howe, C. L., and M. S. Mooseker. 1983. Characterization of the 110-kdalton actin-, calmodulin-, and membrane-binding protein from microvilli of intestinal epithelial cells. *J. Cell Biol.* 97:974–985.
32. Jacobson, K., E. Elson, D. Koppel, and W. Webb. 1983. International workshop on the application of fluorescence photobleaching techniques to problems in cell biology. *Fed. Proc.* 42:72–79.
33. Jacobson, K., A. Ishihara, and R. Inman. 1987. Lateral diffusion of proteins in membranes. *Annu. Rev. Physiol.* 49:163–175.
34. Jesaitis, A. J., and J. Yguerabide. 1986. Lateral mobility of the (Na^+-K^+)ATPase in Madin-Darby canine kidney cells. *J. Cell Biol.* 102: 1256–1263.
35. Kohler, G., and C. Milstein. 1975. Continuous culture of fused cells secreting antibody of pre-defined specificity. *Nature (Lond.).* 256:495–497.
36. Liu, S.-C., L. H. Derick, and J. Palek. 1987. Visualization of the hexagonal lattice in the erythrocyte membrane skeleton. *J. Cell Biol.* 104: 527–536.
37. Livneh, E., M. Benveniste, R. Prywes, S. Felder, Z. Kam, and J. Schlessinger. 1986. Large deletions in the cytoplasmic kinase domain of the epidermal growth factor receptor do not affect its lateral mobility. *J. Cell Biol.* 103:327–331.
38. Lorand, L., L. B. Weissmann, D. L. Epel, and J. Bruner-Lorand. 1976. Role of the intrinsic transglutaminase in the Ca^{++}-mediated crosslinking of erythrocyte proteins. *Proc. Natl. Acad. Sci. USA.* 73:4479–4481.
39. Machamer, C. E., and J. K. Rose. 1987. A specific transmembrane domain of a coronavirus E1 glycoprotein is required for its retention in the Golgi region. *J. Cell Biol.* 105:1205–1214.
40. Maher, P. A., and S. J. Singer. 1985. Anomalous interaction of the acetylcholine receptor protein with the non-ionic detergent Triton X-114. *Proc. Natl. Acad. Sci. USA.* 77:4132–4136.
41. Matlin, K. S., and K. Simons. 1984. Sorting of an apical plasma membrane glycoprotein occurs before it reaches the cell surface in cultured epithelial cells. *J. Cell Biol.* 99:2131–2139.
42. Matlin, K. S., D. Bainton, M. Pesonen, N. Genty, D. Louvard, and K. Simons. 1983. Transfer of a viral envelope glycoprotein from the apical to the basolateral plasma membrane of MDCK cells. I. Morphological evidence. *J. Cell Biol.* 97:627–637.
43. Matsudaira, P. T., and D. R. Burgess. 1979. Identification and organization of the components in the isolated microvillus cytoskeleton. *J. Cell Biol.* 83:667–673.
44. Meza, I., G. Ibarra, M. Sabanero, A. Martinez-Palomo, and M. Cereijido. 1980. Occluding junctions and cytoskeletal components in a cultured transporting epithelium. *J. Cell Biol.* 87:746–754.
45. Misek, D. E., E. Bard, and E. Rodriguez-Boulan. 1984. Biogenesis of epithelial cell polarity: intracellular sorting and vectorial exocytosis of an apical plasma membrane glycoprotein. *Cell.* 39:537–546.
46. Mooseker, M. S. 1985. Organization, chemistry and assembly of the cytoskeletal apparatus of the intestinal brush border. *Annu. Rev. Cell Biol.* 1:209–241.
47. Munro, S., and H. R. B. Pelham. 1987. A C-terminal signal prevents secretion of luminal ER proteins. *Cell.* 48:899–907.
48. Nelson, W. J., and P. J. Veshnock. 1986. Dynamics of membrane-skeleton (fodrin) organization during development of polarity in Madin-Darby canine kidney epithelial cells. *J. Cell Biol.* 103:1751–1766.
49. Nelson, W. J., and P. J. Veshnock. 1987. Modulation of fodrin (membrane skeleton) stability by cell-cell contact in Madin-Darby canine kidney epithelial cell. *J. Cell Biol.* 104:1527–1537.
50. Nelson, W. J., and P. J. Veshnock. 1987. Ankyrin binding to (Na^+ + K^+)ATPase and implications for the organization of membrane domains in polarized cells. *Nature (Lond.).* 328:533–536.
51. Nigg, E. A., and R. J. Cherry. 1980. Anchorage of band 3 population at the erythrocyte cytoplasmic membrane surface: protein rotational diffusion measurements. *Proc. Natl. Acad. Sci. USA.* 77:4702–4706.
52. Nose, A., and M. Takeichi. 1986. A novel cadherin cell adhesion molecule: its expression patterns associated with implantation and organogenesis of mouse embryos. *J. Cell Biol.* 103:2649–2658.
53. Paabo, S., B. M. Bhat, W. S. M. Wold, and P. A. Peterson. 1987. A short sequence in the COOH-terminus makes an adenovirus membrane glycoprotein a resident of the endoplasmic reticulum. *Cell.* 50:311–317.
54. Pesonen, M., and K. Simons. 1983. Transepithelial transport of a viral membrane glycoprotein implanted into the apical plasma membrane of Madin-Darby canine kidney cells. II. Immunological quantitation. *J. Cell Biol.* 97:638–643.
55. Pfeiffer, S., S. D. Fuller, and K. Simons. 1985. Intracellular sorting and basolateral appearance of the G protein of vesicular stomatitis virus in Madin-Darby canine kidney cells. *J. Cell Biol.* 101:470–476.
56. Pisam, M., and P. Ripoche. 1976. Redistribution of surface macromolecules in dissociated epithelial cells. *J. Cell Biol.* 71:907–920.
57. Pollerberg, G. E., M. Schachner, and J. Davoust. 1986. Differentiation state-dependent surface mobilities of two forms of the neural cell adhesion molecules. *Nature (Lond.).* 324:463–465.
58. Rindler, M. J., I. E. Ivanov, H. Plesken, and D. D. Sabatini. 1985. Polarized delivery of viral glycoproteins to the apical and basolateral plasma membranes of Madin-Darby canine kidney cells infected with temperature-sensitive viruses. *J. Cell Biol.* 100:136–151.
59. Rodman, J. S., M. Mooseker, and M. G. Farquhar. 1986. Cytoskeletal proteins of the rat kidney proximal tubule brush border. *Eur. J. Cell Biol.* 42:319–327.
60. Rodriguez-Boulan, E. 1983. Membrane biogenesis: enveloped RNA viruses and epithelial polarity. *Mod. Cell Biol.* 1:119–170.
61. Rodriguez-Boulan, E., K. Paskiet, P. J. I. Salas, and E. Bard. 1984. Intracellular transport of influenza virus hemagglutinin to the apical surface of Madin-Darby canine kidney cells. *J. Cell Biol.* 98:308–319.
62. Rothman, J. E. 1987. Protein sorting by selective retention in the endoplasmic reticulum and Golgi stack. *Cell.* 50:521–522.
63. Salas, P. J. I., D. E. Misek, D. E. Vega-Salas, D. Gundersen, M. Cereijido, and E. Rodriguez-Boulan. 1986. Microtubules and actin microfilaments are not critically involved in the biogenesis of epithelial cell surface polarity. *J. Cell Biol.* 102:1853–1867.
64. Salas, P. J. I., D. E. Vega-Salas, D. E. Misek, E. Bard, and E. Rodriguez-Boulan. 1984. Intracellular sorting of plasma membrane glycoproteins in epithelial cells. *Ann. NY Acad. Sci.* 435:337–340.
65. Salas, P. J. I., D. E. Vega-Salas, and E. Rodriguez-Boulan. 1987. Collagen receptors mediate early events in the attachment of epithelial (MDCK) cells. *J. Membr. Biol.* 98:223–236.
66. Scullion, B. F., Y. Hou, L. Puddington, J. K. Rose, and K. Jacobson. 1987. Effects of mutations in three domains of the vesicular stomatitis viral glycoprotein on its lateral diffusion in the plasma membrane. *J. Cell Biol.* 105:69–75.
67. Sheetz, M. P. 1979. Integral membrane protein interaction with Triton cytoskeletons of erythrocytes. *Biochim. Biophys. Acta.* 557:122–134.
68. Sheetz, M. P., M. Schindler, and D. E. Koppel. 1980. Lateral mobility of integral membrane proteins is increased in spherocytic erythrocytes. *Nature (Lond.).* 285:510–511.
69. Siefring, G. E., A. B. Apostol, P. T. Velasco, and L. Lorand. 1978. Enzymatic basis for the Ca^{++}-induced cross-linking of membrane proteins in intact human erythrocytes. *Biochemistry.* 17:2598–2604.
70. Simons, K., and S. D. Fuller. 1985. Cell surface polarity in epithelia. *Annu. Rev. Cell Biol.* 1:243–288.
71. Singer, S. J., and G. L. Nicolson. 1972. The fluid mosaic model of the structure of cell membranes. *Science (Wash.).* 175:720–731.
72. Slife, C. W., M. D. Dorsett, and M. L. Tillotson. 1986. Subcellular location and identification of a large molecular weight substrate for the liver plasma membrane transglutaminase. *J. Biol. Chem.* 261:3451–3456.
73. Smith, D. K., and J. Palek. 1982. Modulation of lateral mobility of band

3 in the red cell membrane by oxidative cross-linking of spectrin. *Nature (Lond.)*. 297:424–425.
74. Deleted in proof.
75. Steinberg, M. S., H. Shida, G. J. Giudice, M. Shida, N. H. Patel, and O. W. Blaschuk. 1987. On the molecular organization, diversity and functions of desmosomal proteins. *Ciba Found. Symp.* 125:3–25.
76. Stevenson, B. R., J. D. Siliciano, M. S. Mooseker, and D. A. Goodenough. 1986. Identification of ZO-1: a high molecular weight polypeptide associated with the tight junction (zonula occludens) in a variety of epithelia. *J. Cell Biol.* 103:755–766.
77. Deleted in proof.
78. Tarone, G., R. Ferrachini, G. Galetto, and P. Comoglio. 1984. A cell surface integral membrane glycoprotein of 85,000 mol wt (gp85) associated with Triton X-100 insoluble cell skeleton. *J. Cell Biol.* 99:512–519.
79. Tsuji, A., and S. Ohnishi. 1986. Restriction of the lateral motion of band 3 in the erythrocyte membrane by the cytoskeletal network: dependence on spectrin association state. *Biochemistry.* 25:6133–6139.
80. Tyrrell, D. J., W. S. Sale, and C. W. Slife. 1986. Localization of a liver transglutaminase and a large molecular weight transglutaminase substrate to a distinct plasma membrane domain. *J. Biol. Chem.* 261:14833–14836.
81. van Meer, G., and K. Simons. 1986. The function of tight junctions in maintaining differences in lipid composition between the apical and the basolateral cell surface domains of MDCK cells. *EMBO (Eur. Mol. Biol. Org.) J.* 5:1455–1464.
82. Vega-Salas, D. E., P. J. I. Salas, D. Gundersen, and E. Rodriguez-Boulan. 1987. Formation of the apical pole of epithelial Madin-Darby canine kidney cells: polarity of an apical protein is independent of tight junctions while segregation of a basolateral marker requires cell–cell interactions. *J. Cell Biol.* 104:905–916.
83. Vega-Salas, D. E., P. J. I. Salas, and E. Rodriguez-Boulan. 1987. Modulation of the expression of an apical plasma membrane protein of Madin-Darby Canine Kidney epithelial cells: cell–cell interactions control the appearance of a novel intracellular storage compartment. *J. Cell Biol.* 104:1249–1259.
84. Vega-Salas, D. E., P. J. I. Salas, and E. Rodriguez-Boulan. 1988. Exocytosis of Vacuolar Apical Compartment (VAC): a cell–cell contact controlled mechanism for the establishment of the apical plasma membrane domain in epithelial cells. *J. Cell Biol.* 107:1717–1728.
85. Deleted in proof.
86. Wier, M. L., and M. Edidin. 1986. Effects of cell density and extracellular matrix on the lateral diffusion of major histocompatibility antigens in cultured fibroblasts. *J. Cell Biol.* 103:215–222.
87. Wolf, D. E., A. H. Handyside, and M. Edidin. 1982. Effect of microvilli on lateral diffusion measurements made by the fluorescence photobleaching recovery technique. *Biophys. J.* 38:295–297.
88. Ziomek, C. A., S. Schulman, and M. Edidin. 1980. Redistribution of membrane proteins in isolated mouse intestinal epithelial cells. *J. Cell Biol.* 86:849–857.